# High electric field transport in $In_{0.53}Ga_{0.47}As$ quantum wells under nonquantizing magnetic fields at low temperatures

S. K. Sarkar[1] and D. Chattopadhyay[2]
[1]*Department of Electronics and Telecommunication Engineering, Jadavpur University, Calcutta 700032, India*
[2]*Institute of Radiophysics and Electronics, University of Calcutta, 92 Acharya Prafulla Chandra Road, Calcutta 700009, India*
(Received 7 December 1999; revised manuscript received 28 September 2000)

Hall mobility, magnetoresistance coefficient, and Hall-to-drift mobility ratio of two-dimensional hot electrons in $In_{0.53}Ga_{0.47}As$ square quantum wells are calculated for classical magnetic fields for lattice temperatures in the range 4–15 K considering the degeneracy of the distribution function and incorporating screened deformation-potential acoustic, ionized impurity, and alloy disorder scattering. The variations of the galvanomagnetic coefficients with the channel width, the lattice temperature, and the electric and magnetic fields are studied. The magnetoresistance is found to change more remarkably than the Hall mobility or the Hall ratio with changes in the lattice temperature, the channel width, and the electric and magnetic fields.

The optical and the transport properties of two-dimensional (2D) electron gas in $In_{0.53}Ga_{0.47}As$ have attracted much attention in recent years, including their applications in modern devices.[1] Galvanomagnetic transport in (In,Ga)As quantum wells (QW's) under Ohmic electric fields was investigated earlier by Ghosh and Chattopadhyay.[2] But studies for a high heating electric field and a crossed low nonquantizing magnetic field are scarce in the literature, particularly for (In,Ga)As QW's. In this paper, we calculate the galvanomagnetic transport coefficients viz. Hall mobility, Hall-to-drift mobility ratio, and magnetoresistance coefficient of 2D hot electrons in a square QW of (In,Ga)As for nonquantizing magnetic fields for lattice temperatures in the range of 4–15 K in the framework of the heated Fermi-Dirac distribution function. Low lattice temperatures are preferred because the electron mobility is enhanced due to the reduction of phonon scattering and the suppression of ionized impurity scattering caused by modulation doping.[3] Also, at low temperatures, noise and energy spread of electrons involved in the transport are reduced substantially.[4] The effects of changes in the channel width, the lattice temperature, and the electric and magnetic fields on the galvanomagnetic transport coefficients are studied here.

A square QW of (In,Ga)As with infinite barrier height and of width $L_z$ is considered. The carriers are assumed to occupy the lowest subband only. Over the range of lattice temperatures, the channel width, and the 2D carrier concentration considered here, the separation between the first excited state and the ground quantum state is found to be at least four times the average carrier energy at the highest heating electric field, thus justifying the foregoing assumptions.

Screened carrier scattering via deformation-potential acoustic, background impurities, and alloy disorder are considered as they are the major scattering mechanisms at low temperatures.[5] The energy loss at higher electron temperatures is dominated by longitudinal-optic (LO) phonons,[6] the treatment of which must include several complexities that are not yet fully resolved.[7] However, the heating electric fields and lattice temperatures considered here are such that the electron temperature is always below 30 K so that the contribution of LO-phonon scattering is insignificant.[6] Furthermore, the effect of remote impurity scattering is not included here as it can be reduced substantially by introducing a thick spacer layer.[8] The electrons lose energy through deformation-potential acoustic scattering for electron temperatures less than 40 K.[6] The contribution of the piezoelectric scattering is an order of magnitude lower,[6] and hence not included in the calculations here.

In the rectangular Cartesian coordinate system, we take the $z$ axis perpendicular to the interfacial planes so that the carriers are free to move parallel to the $xy$ plane. The classical magnetic field $B$ and the heating electric field $F$ are assumed to act along the $z$ and the $x$ axis, respectively. The reduction of the effect of ionized impurities and improved carrier confinement establish a strong electron-electron interaction in the channel. An electron temperature is, therefore, established in a 2D electron gas system, as revealed in photoluminescence experiments.[9] The carrier distribution function is thus given by

$$f(\mathbf{k}) = f_0(E) + (e\hbar F/m^*)(-\partial f_0/\partial E)[k_x \xi(E) - \omega_B k_y \xi(E)], \tag{1}$$

where $f_0(E)$ is the Fermi-Dirac distribution function at an electron temperature $T_e$. $e$ and $m^*$ are the electronic charge and effective mass, respectively, $\hbar$ is the Planck's constant divided by $2\pi$, $\omega_B$ $(=eB/m^*)$ is the cyclotron angular frequency, $k_x$ and $k_y$ are the $x$ and $y$ components of the 2D wave vector $\mathbf{k}$ for the electron energy $E$, and $\xi_x$ and $\xi_y$ are the perturbation functions. As streaming of the distribution function is not important and the scattering processes are not mainly in the forward direction, the two-term Legendre polynomial expansion of $f$ is used here.

The heating electric field $F$ and the electron temperature $T_e$ are related through the energy balance equation:

$$\int E(\partial f/\partial t)_{\text{field}} d\mathbf{k} + \int E(\partial f/\partial t)_{\text{coll}} d\mathbf{k} = 0. \tag{2}$$

For inelastic screened deformation-potential acoustic scattering, $(\partial f/\partial t)_{\text{coll}}$ is obtained from the square of the relevant

 

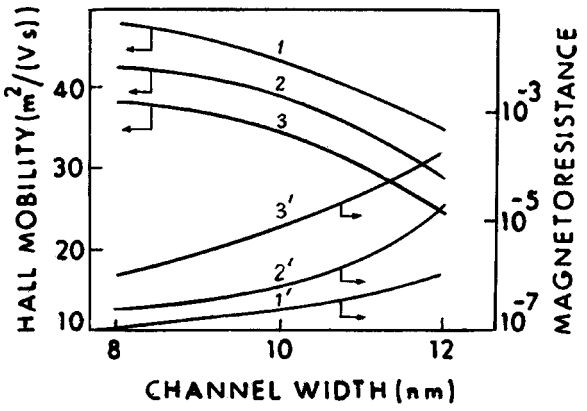


FIG. 1. Variation of Hall mobility ($\mu_H$) and magnetoresistance ($R_m$) with the channel width ($L_z$) for a nonquantizing magnetic field of 0.001 T for a lattice temperature 4 K, 2D carrier concentration ($n_{2D}$) of $6\times10^{15}\,\mathrm{m}^{-2}$ and impurity concentration ($n_{bi}$) of $6\times10^{21}\ \mathrm{m}^{-3}$. (1),(1′): $E=250$ V/m; (2),(2′): $E=500$ V/m; (3),(3′): $E=750$ V/m.

matrix element for the 2D system[10] following the procedure similar to that used for the bulk material.[11] Thus $f_0(E+\hbar\omega_q)$ is expanded in a Taylor series and the terms with powers higher than 2 are neglected, the acoustic-phonon energy $\hbar\omega_q$ being much less than the carrier energy $E$. The integrations are carried out numerically over the in-plane and the perpendicular components of the 3D phonon wave vector $\mathbf{Q}$ retaining only the highest-order terms in $m^*u_l/\hbar$, where $u_l$ is the longitudinal acoustic velocity.

The perturbation functions, determined from the Boltzmann transport equation, are given by

$$\xi_x(E)=\tau(E)/[1+\omega_B^2\tau^2(E)], \tag{3}$$

$$\xi_y(E)=\tau(E)\xi_x(E). \tag{4}$$

Here, $\tau(E)$ is the momentum relaxation time given by

$$\tau^{-1}(E)=\tau_{\mathrm{ac}}^{-1}(E)+\tau_{\mathrm{imp}}^{-1}(E)+\tau_{\mathrm{al}}^{-1}(E), \tag{5}$$

where $\tau_{\mathrm{ac}}(E)$, $\tau_{\mathrm{imp}}(E)$, and $\tau_{\mathrm{al}}(E)$ are, respectively, the momentum relaxation times for acoustic, ionized impurity, and alloy scattering. The detailed expressions for $\tau_{\mathrm{ac}}(E)$, $\tau_{\mathrm{imp}}(E)$, and $\tau_{\mathrm{al}}(E)$ are, respectively, found in Refs. 12, 13, and 14. The Hall mobility ($\mu_H$), the magnetoresistance coefficient ($R_m$), and the Hall-to-drift mobility ratio ($r_H$) are expressed by

$$\mu_H=(\mu_{xx}(0)|\mu_{xy}|)/B(\mu_{xx}^2+\mu_{xy}^2), \tag{6}$$

$$R_m=(B\mu_{xx}\mu_H/\mu_{xy}-1), \tag{7}$$

$$r_H=\mu_H/\mu_{xx}(0), \tag{8}$$

where

$$\mu_{xx}=A\int E\xi_x(E)(-\partial f_0/\partial E)dE, \tag{9}$$

$$\mu_{xy}=A\omega_B\int E\xi_y(E)(-\partial f_0/\partial E)dE. \tag{10}$$

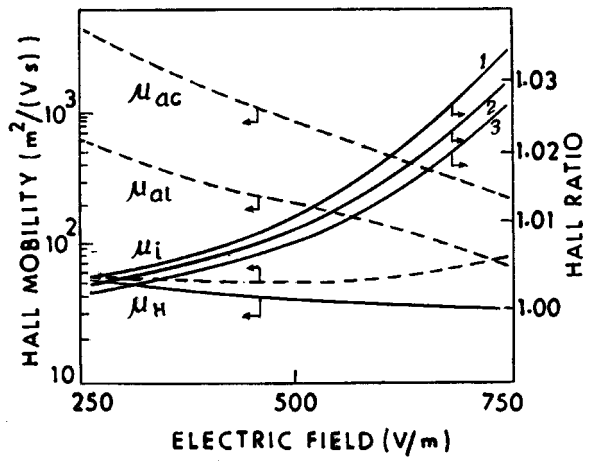


FIG. 2. Plots of Hall mobility ($\mu_H$) and Hall-to-drift mobility ratio ($r_H$) vs electric field for a typical channel width of 10 nm at a lattice temperature of 4 K with the parameters of Fig. 1. The contributions of various scattering mechanisms acting separately are shown. (1): $B=0.001$ T; (2): $B=0.005$ T; (3): $B=0.01$ T.

Here $A=e/(\hbar^2\pi n_{2D})$ and $\mu_{xx}(0)$ is the value of $\mu_{xx}$ for $B=0$.

Figure 1 depicts the variation of Hall mobility ($\mu_H$) and magnetoresistance coeffcient ($R_m$) with the channel width ($L_z$) for a nonquantizing magnetic field of 0.001 T at electric fields of 250, 500, and 750 V/m for a lattice temperature of 4 K. Typical values of $6\times10^{15}\,\mathrm{m}^{-2}$ for 2D carrier concentration ($n_{2D}$) and $6\times10^{21}\,\mathrm{m}^{-3}$ for impurity concentration ($n_{bi}$) are used here in the calculations. $\mu_H$ decreases and $R_m$ increases with $L_z$. This nature of variation is linked with the fact that as $L_z$ increases, the phonon scattering becomes weaker[12] and the impurity scattering gets stronger.[13] $\mu_H$ is lower and $R_m$ is higher at higher electric fields. When $L_z$ is increased from 8 to 12 nm, $\mu_H$ decreases by 25% at 250 V/m, 30% at 500 V/m, and 35% at 750 V/m. But the increase of $R_m$ is more than an order of magnitude in all the cases considered here.

Figure 2 shows the calculated electric field dependence of

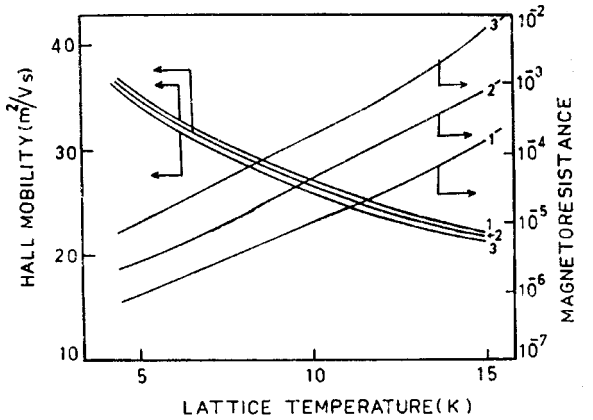


FIG. 3. Plots of Hall mobility ($\mu_H$) and magnetoresistance ($R_m$) vs lattice temperature for a typical electrical field of 500 V/m and channel width of 10 nm. The other parameters are the same as in Fig. 1. (1),(1′): $B=0.001$ T; (2),(2′): $B=0.005$ T; (3),(3′): $B=0.01$ T.

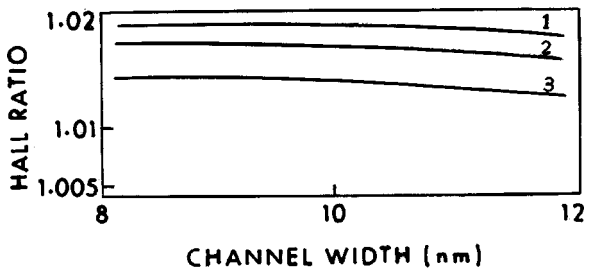


FIG. 4. Plots of Hall-to-drift mobility ratio ($r_H$) vs channel width ($L_z$) for a typical electric field of 500 V/m and magnetic field of 0.001 T. The other parameters are the same as in Fig. 1. (1): $T_L=4$ K; (2): $T_L=10$ K; (3): $T_L=15$ K.

Hall mobility ($\mu_H$) and the Hall-to-drift mobility ratio ($r_H$) for a typical channel width of 10 nm at a lattice temperature of 4 K. The other parameters are the same as in Fig. 1. The contributions of the various scattering mechanisms acting separately are depicted in the figure. The mobilities limited by deformation-potential acoustic and alloy disorder scatterings are found to decrease with increasing electric field due to the enhancement of electron temperature. The ionized impurity-limited mobility, however, increases with the increase of the electric field due to its Coulombic nature. The overall mobility (solid curve) is dominated by the ionized impurity scattering, which is the major mechanism in determining the Hall mobility. The Hall ratio increases with the electric field due to the combined scattering mechanisms, but it is not larger than 1.04. Hence, the replacement of the Hall mobility by the drift mobility will not introduce great errors. The Hall ratio also decreases with the increase of the magnetic field.

The variations of $\mu_H$ and $R_m$ with the lattice temperature for a typical electric field of 500 V/m and channel width of 10 nm with the parameter values of Fig. 1 are shown in Fig. 3. $\mu_H$ decreases and $R_m$ increases with the rise of lattice temperature ($T_L$). $R_m$ is found to be very sensitive to the changes in $B$. But the Hall mobility $\mu_H$ is quite insensitive to a change in $B$. We find that as $B$ is reduced from 0.01 to 0.001 T, $\mu_H$ changes by 2% to 3% only. As the lattice temperature increases, the phonon scattering gets stronger due to the increase of the phonon occupation number, thereby decreasing $\mu_H$.

The variation of the Hall ratio with the channel width for different lattice temperatures is depicted in Fig. 4. The other parameters are the same as in Fig. 1. From Fig. 4 it is evident that the Hall ratio remains almost constant with the variation of channel width ($L_z$). The Hall ratio is very close to unity at low lattice temperatures as a result of the strong degeneracy of the carrier distribution function.

In conclusion, the magnetoresistance is found to be more sensitive than $\mu_H$ or $r_H$ to the changes in the lattice temperature, the channel width, and the magnetic and the electric fields. Thus the experimental measurements of $R_m$ would shed more light on the scattering rates controlling the carrier kinetics in (In,Ga)As QW's.

[1] R. Kyburz, J. Schmid, R. S. Popovic, and H. Melchior, IEEE Trans. Electron Devices **41**, 315 (1994).
[2] P. K. Ghosh and D. Chattopadhyay, Phys. Status Solidi B **184**, 171 (1994).
[3] H. L. Stormer, J. Phys. Soc. Jpn. Suppl. A **49**, 1013 (1980).
[4] S. Dutta and M. J. Mclennan, Rep. Prog. Phys. **53**, 1003 (1980).
[5] P. K. Ghosh and D. Chattopadhyay, Phys. Rev. B **48**, 17 177 (1993).
[6] K. Hirakawa and H. Sakaki, Appl. Phys. Lett. **49**, 889 (1986).
[7] J. A. Brun and G. Bastard, Solid State Commun. **53**, 727 (1985).
[8] J. J. Haris, C. T. Foxon, D. F. Lucklison, and K. W. J. Barnham, Superlattices Microstruct. **2**, 563 (1986).
[9] J. Shah, A. Pinezuk, A. C. Gossard, and W. Wiegmann, Phys. Rev. Lett. **51**, 45 (1985).
[10] P. J. Price, Ann. Phys. (N.Y.) **133**, 217 (1981).
[11] E. M. Conwell, *High Field Transport in Semiconductors* (Academic, New York, 1967).
[12] D. Chattopadhyay, Phys. Status Solidi B **135**, 409 (1986).
[13] J. Lee, H. N. Spectra, and V. K. Arora, J. Appl. Phys. **54**, 6995 (1983).
[14] D. Chattopadhyay, Appl. Phys. A: Solids Surf. **53**, 35 (1991).